

Coupled effects of local movement and global interaction on contagion

Li-Xin Zhong^{a,b}, Wen-Juan Xu^c, Rong-Da Chen^a, Tian Qiu^d, Chen-Yang Zhong^e

^a*School of Finance and Coordinated Innovation Center of Wealth Management and Quantitative Investment, Zhejiang University of Finance and Economics, Hangzhou, 310018, China*

^b*School of Economics and Management, Tsinghua University, Beijing, 100084, China*

^c*School of Law, Zhejiang University of Finance and Economics, Hangzhou, 310018, China*

^d*School of Information Engineering, Nanchang Hangkong University, Nanchang, 330063, China*

^e*Yuanpei College, Peking University, Beijing, 100871, China*

Abstract

By incorporating segregated spatial domain and individual-based linkage into the SIS (susceptible-infected-susceptible) model, we investigate the coupled effects of random walk and intragroup interaction on contagion. Compared with the situation where only local movement or individual-based linkage exists, the coexistence of them leads to a wider spread of infectious disease. The roles of narrowing segregated spatial domain and reducing mobility in epidemic control are checked, these two measures are found to be conducive to curbing the spread of infectious disease. Considering heterogeneous time scales between local movement and global interaction, a log-log relation between the change in the number of infected individuals and the timescale τ is found. A theoretical analysis indicates that the evolutionary dynamics in the present model is related to the encounter probability and the encounter time. A functional relation between the epidemic threshold and the ratio of shortcuts, and a functional relation between the encounter time and the timescale τ are found.

Keywords: local movement, individual-based linkage, multi-layer network, SIS model

Email address: zlxxwj@163.com (Li-Xin Zhong^{a,b})

1. Introduction

Over the past two decades, the world has witnessed the threat of infectious disease with long-range transmission, such as the severe acute respiratory syndrome (SARS), the pandemic Influenza A (H1N1) and the 2014 Ebola epidemic. Understanding the reaction-diffusion processes in complex systems and finding an effective way to prevent and control the outbreak of infectious disease have become an urgent but difficult challenge[1].

In modelling the propagation of infectious disease, the susceptible-infected-susceptible (SIS) model and the susceptible-infected-recovered (SIR) model represent two distinctive disease transmission processes[2, 3, 4]. In the SIS model, each individual is initially in one of the two states: S (susceptible) and I (infected). A susceptible individual may become infected as he encounters an infected individual, and an infected individual may become susceptible again after some time. In the SIR model, each individual is initially in one of the three states: S, I and R (recovered). The only difference between the SIS model and the SIR model is that, in the SIR model, an infected individual firstly becomes healthy (recovered), when he is immune to the disease. After some time, the recovered individual may become susceptible to the disease again.

The spread of infectious disease is closely related to mobility patterns and interaction patterns of the population[5, 6, 7, 8]. An individual may move about aimlessly like a floating boat in the ocean or travel along a certain path like a move on the chessboard. Two individuals may interact with each other day after day because they are in the same firm or only have a chance encounter because neither of them likes establishing a fixed relationship with any other people. To understand the roles of underlying structure in the evolution of collective behaviors, different network models are usually borrowed to simulate the mobility patterns and the interaction patterns[9, 10, 11, 12, 13, 14, 15]. The existing network models can be classified into two families: the network with a single layer, including regular network, random network and scale-free network[16, 17, 18, 19], and the network with multiple-layers[20, 21, 22, 23], which consists of two or more sub-networks.

Z.H. Liu et al. have investigated the roles of community structure in epidemic propagation[24, 25, 26, 27], they have found that the existence of

community structure leads to a smaller threshold of epidemic outbreak. Z.M. Yang et al. have studied the effect of connection patterns on the outbreak of epidemic, they have found that a heterogeneous network structure accelerates the spread of infectious disease[28, 29, 30, 31]. K. P. Chan et al. have investigated the effects of aging and links removal on epidemic spread in scale-free networks, the local and global spreads are found to be related to the number of links removed[32]. M. Dickison et al. have studied the epidemic spreading on interconnected networks, a global endemic state is found to be related to the strongly-coupled or weakly-coupled network systems[33]. X. F. Fu et al. have studied the effect of mobility patterns on the outbreak of epidemic, they have found that the change of encounter probability, which may result from the change of population density or the change of moving probability, plays an important role in the change of infected individuals[34, 35]. V. Colizza et al. have investigated the invasion dynamics in metapopulation systems, they have found that the heterogeneous connectivity and the mixed mobility pattern play an important role in the outbreak of epidemic [36].

Until today, in relation to the roles of mobility patterns and connection patterns in the outbreak of epidemic, most of the studies consider the two factors respectively. However, in the real world, the evolutionary dynamics in reaction-diffusion systems is usually determined by the coupling of mobility and connectivity, especially the group dynamics in social and economic systems [37, 38, 39, 40, 41]. For example, a susceptible individual may be infected by an unknown individual in a random walk after dinner or be infected by a business partner. The coupled effects of random walk and pre-arranged interaction on contagion are short of in-depth study. In relation to the measures for disease control and prevention, most of the studies focus on the effects of immunization and isolation, which especially rely on the knowledge of one's activity routine and one's friendship network. Generally speaking, compared with the route of random walk, a predefined interaction structure is much easier to be understood. In view of the coupling of random walk and predefined interaction structure, the effect of local activity restriction on global epidemic suppression is worth extra attention.

Take localized random walk and individual-based global interaction into consideration, in the present model, we incorporate a multi-layer network, which consists of a regular network with segregated spatial domains and a random network representing individual-based linkage, into the SIS model. The coupled dynamics of random walk and intragroup interaction is investigated, and the roles of narrowing segregated spatial domain and reducing

mobility in epidemic control are checked. The following are our main findings.

(1) Compared with the situation where only localized random walk or individual-based linkage exists, the coexistence of local movement and global interaction leads to a higher ratio of infected individuals.

(2) The size of segregated spatial domain plays an important role in the outbreak of epidemic. As both the spatial size and the population size are given, narrowing the segregated spatial domain not only slows down the spread of infectious disease but also leads to a decrease in the number of infected individuals in the final steady state.

(3) Local mobility has a great impact on the global spread of infectious disease. On condition that there is little individual-based connection, reducing local mobility can effectively suppress the global spread of epidemic.

(4) A theoretical analysis indicates that the outbreak of epidemic is related to the encounter probability and the encounter time. The existence of shortcuts leads to an increase in encounter probability and therefore a decrease in the number of infected individuals. Narrowing segregated spatial domain leads to an increase in encounter time and therefore a decrease in the number of infected individuals. A functional relation between the epidemic threshold and the ratio of shortcuts, and a functional relation between the encounter time and the timescale τ are found.

The rest of the paper is organized as follows. The SIS model with a multi-layer network is introduced in section two. In section three, simulation results are presented and discussed in detail. The epidemic dynamics is theoretically analyzed in section four and conclusions are drawn in section five.

2. The model

In the present model, each individual has two possible activities: acting as a random walker whose activity domain is restricted to a given local area and acting as a businessman whose activity is confined to interacting with his familiars. To model the evolutionary dynamics in local movement and global (intragroup) interaction respectively, we incorporate a multi-layer network with two subnetworks, which are called mobility network and interaction network respectively throughout the paper, into the SIS model.

The mobility network is a regular network with $L \times L$ sites, each of which has eight connected neighbor sites. The overall spatial domain is divided into $N_{local} = \frac{L}{d_x - \Delta d_x} \times \frac{L}{d_y - \Delta d_y}$ segregated spatial domains. The area of each

domain is $s = d_x \times d_y$ and the overlapping area of two nearby domains is $\Delta s = d_y \times \Delta d_x$ or $d_x \times \Delta d_y$. There are total N ($\leq L \times L$) individuals staying on the sites of the mobility network, each of whom can move along the link between the sites but is not allowed to walk out of the segregated spatial domain which is randomly allocated to each individual at the initial time.

The interaction network is a random network with N sites and $(N - 1)\phi$ links on average for each site. Different sites denote different individuals and the links between sites denote social relations between the individuals. The intragroup interactions only take place between the individuals with immediate connections.

The reaction-diffusion process in the multi-layer network is as follows. There exists a timescale τ between global interaction and local movement. At each time step, an agent i firstly makes his decision whether to interact with his familiar or go for a random walk. He makes intragroup interaction with probability τ and makes local movement with probability $1 - \tau$. In the process of local movement, agent i firstly makes his decision whether to move or not with probability v . If he chooses "Yes", he randomly chooses a neighbor site from the total nine connected sites to stay on. If the chosen site is outside the local area, he does not move. If he chooses "No", he does not make a movement. After the movement decision has been made, for an infected individual, he becomes susceptible with probability p_s . For a susceptible individual, he becomes infected with probability $\frac{n_I}{n_s + n_I} p_I$, in which n_s and n_I are the number of susceptible individuals and infected individuals respectively and $n_s + n_I$ is the total number of individuals on the same site. In the process of intragroup interaction, agent i firstly chooses an agent j from his connected neighbors. Then, if agent i is an infected individual, he becomes susceptible with probability p_s . If agent i is a susceptible individual and agent j is an infected individual, agent i becomes infected with probability p_I . The updating is made asynchronously.

Therefore, in the present model, the mobility network and the interaction network are coupled by the individuals, and the local epidemic dynamics and the global epidemic dynamics are coupled by the time scale τ . For $0.5 < \tau \leq 1$, the global interaction process is faster than the local interaction process. For $\tau = 0.5$, the global interaction process is the same as the local interaction process. For $0 \leq \tau < 0.5$, the global interaction process is slower than the local interaction process.

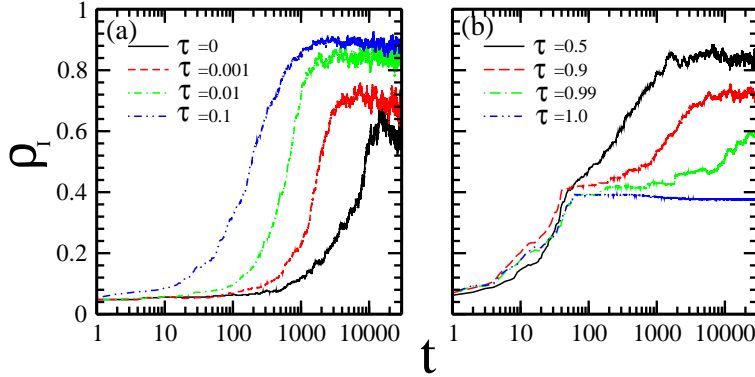


Figure 1: The time-dependent ratio of infected individuals for a system with $N = 500$, $p_I = 1$, $p_s = 0.001$, $d_x = d_y = 11$, $v = 0.05$, $\phi = 0.002$, (a) $\tau=0$ (line), 0.001 (slash), 0.01 (slash dotted), 0.1 (slash dotted dotted); (b) $\tau=0.5$ (line), 0.9 (slash), 0.99 (slash dotted), 1 (slash dotted dotted).

3. Simulation results and discussions

In the present model, we especially care about the coupled effects of local movement and global interaction. Throughout the paper, the following parameters are given. The overlapping size is $\Delta d_x = \Delta d_y = 1$, the overall spatial size is $L \times L = 100 \times 100$, the initial ratio of infected individuals $\rho_I = 0.05$. To reduce the influence of boundary effect, the segregated spatial domain is given as a square domain, that is, $d_x = d_y$.

In figure 1 (a) and (b) we give the time-dependent ratio of infected individuals ρ_I for a fixed ratio of shortcuts $\phi = 0.002$ and different time scale τ . Figure 1 (a) shows that, for $\tau=0$, which corresponds to the situation where the contact between different individuals only results from random walk, ρ_I increases slowly with the time and finally reaches an intermediate level of $\rho_I \sim 0.6$. As τ increases from $\tau = 0.001$ to $\tau = 0.1$, the relaxation time decreases while the ratio of infected agents in the final steady states increases with the rise of τ . The smaller the value of τ , the more sensitive of ρ_I to the change in τ .

Different from the results in figure 1 (a), figure 1 (b) shows that, as τ increases from $\tau = 0.5$ to $\tau = 0.99$, the relaxation time increases while the ratio of infected agents in the final steady states decreases with the rise of τ . The larger the value of τ , the more sensitive of ρ_I to the change in τ . For $\tau=1$, which corresponds to the situation where the contact between different individuals only results from intragroup interaction, the ratio of infected

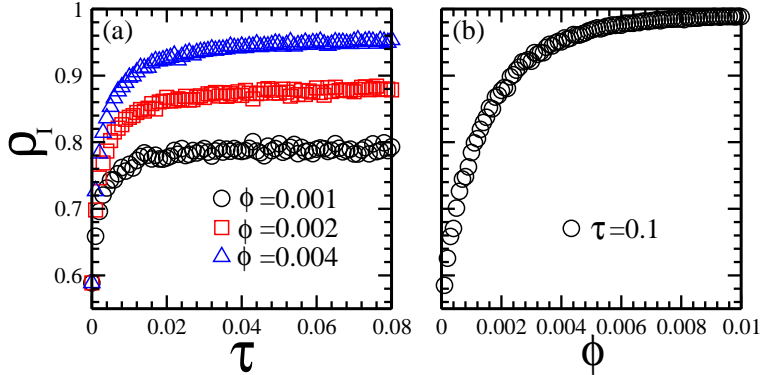


Figure 2: The averaged ratio of infected individuals (a) as a function of timescale τ for the ratio of random connection $\phi=0.001$ (circles), 0.002 (squares), 0.004 (triangles) and (b) as a function of the ratio of random connection ϕ for $\tau = 0.1$. Final results are averaged over 10 runs and 10^4 time steps with 10^5 relaxation time in each run. Other parameters are: $N = 500$, $p_I = 1$, $p_s = 0.001$, $d_x = d_y = 11$, $v = 0.05$.

agents in the final steady state is a low level of $\rho_I \sim 0.37$.

The above results indicate that, compared with the situation where the contact between different individuals only results from random walk or intragroup interaction, when local movement and global interaction coexist, it is much easier for the infectious disease to spread globally.

To find the quantitative relation between ρ_I and τ for a given ϕ and the quantitative relation between ρ_I and ϕ for a given τ , in figure 2 (a), we give ρ_I as a function of τ for $\phi = 0.001, 0.002, 0.004$. In figure 2 (b) we give ρ_I as a function of ϕ for $\tau = 0.1$. Figure 2 (a) shows that, for a small $\phi = 0.001$, within the range of $0 < \tau < 0.02$, ρ_I increases quickly from $\rho_I \sim 0.58$ to $\rho_I \sim 0.78$. Within the range of $\phi > 0.02$, ρ_I changes little with the rise of τ . For $\tau > 0$, an increase in ϕ leads to an overall rise of ρ_I . Figure 2 (b) tells us that, for a given $\tau = 0.1$, only within the range of $0 < \phi < 0.008$, ρ_I is quite sensitive to the change in ϕ . Within the range of $\phi > 0.008$, ρ_I reaches its maximum value and changes little with the rise of ϕ . Such results indicate that, in the scenario where the individuals are confined to segregated spatial domain, the existence of a small number of shortcuts can effectively lead to a rise of the ratio of infected individuals, which is similar to the result found in the small world network[42].

The above results indicate that the evolutionary dynamics in the present model is determined by the mobility pattern and the connection pattern.

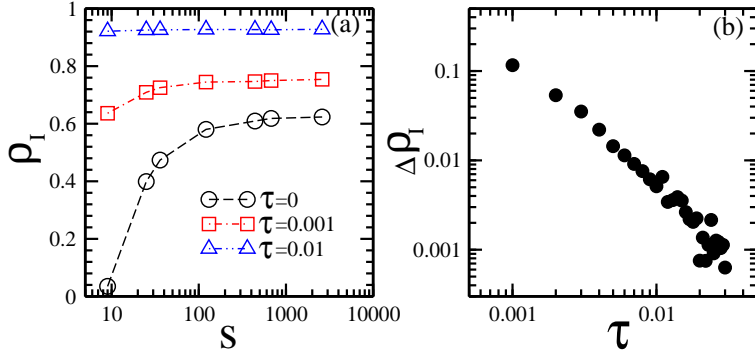


Figure 3: (a) The averaged ratio of infected individuals as a function of the area s of segregated spatial domain for $\phi=0.01$, $\tau=0$ (circles), 0.001 (squares), 0.01 (triangles); (b) The change in the averaged ratio of infected individuals, $\Delta\rho_I = \rho_I^{s=2601} - \rho_I^{s=9}$, as a function of τ . Final results are averaged over 10 runs and 10^4 time steps with 10^5 relaxation time in each run. Other parameters are: $N = 500$, $p_I = 1$, $p_s = 0.001$, $v = 0.05$.

To find out the relationship between local behavior and global behavior, in the following, the effects of three parameters on epidemic control are investigated respectively. The three parameters are: the area of segregated spatial domain s , the frequency of intragroup interaction τ , and the ratio of segregated spatial domains with activity restriction ζ (called slow domain in the following).

Figure 3 (a) displays the averaged ratio of infected individuals ρ_I as a function of s for $\phi = 0.01$ and $\tau = 0, 0.001, 0.1$ respectively. For $\tau=0$, as s increases from $s=9$ to $s=121$, ρ_I increases quickly from $\rho_I \sim 0.04$ to $\rho_I \sim 0.58$. As s increases from $s=121$ to $s=2601$, ρ_I increases slowly and finally reaches its maximum value $\rho_I \sim 0.62$. Increasing τ leads to an overall rise of ρ_I within the whole range of $9 \leq s \leq 2601$. The smaller the value of s , the more sensitive of ρ_I to the change in τ .

The above results indicate that, by narrowing the segregated spatial domain (called activity domain restriction in the following), the epidemic spread may be inhibited, the effect of which depends on whether there exists global interaction or not. A higher frequency of global interaction will make activity domain restriction become less effective. Figure 3 (b) shows the relationship between the change of ρ_I , $\Delta\rho_I = \rho_I^{s=2601} - \rho_I^{s=9}$, and the time scale τ . A log-log relation between $\Delta\rho_I$ and τ , $\Delta\rho_I \sim a\tau^{-b}$, in which $a \sim 4.2 \times 10^{-6}$ and $b \sim 1.53$, is found.

To find out whether local mobility restriction can effectively inhibit the

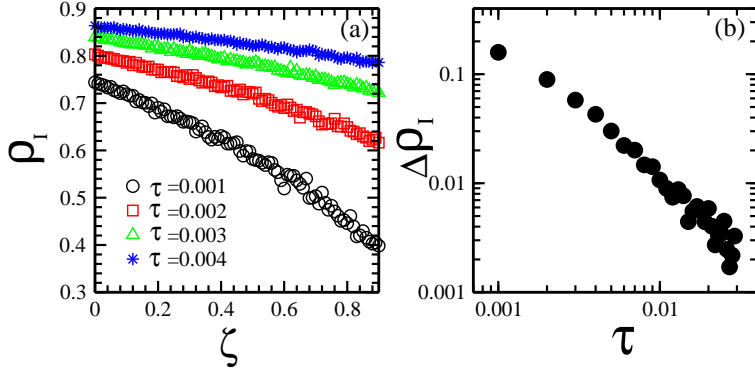


Figure 4: (a) The averaged ratio of infected individuals as a function of the ratio of slow domains ζ for $\phi = 0.01$ and $\tau=0.001$ (circles), 0.002 (squares), 0.003 (triangles), 0.004 (stars); (b) The change in the averaged ratio of infected individuals $\Delta\rho_I = \rho_I^{\zeta=0} - \rho_I^{\zeta=0.5}$ as a function of τ for $\phi=0.01$. Final results are averaged over 10 runs and 10^4 time steps with 10^5 relaxation time in each run. Other parameters are: $N = 500$, $p_I = 1$, $p_s = 0.001$, $d_x = d_y = 11$, $v = 0.05$, $v_{slow} = 0.1v$.

global spread of epidemic, in figure 4 (a) we plot the averaged ratio of infected individuals as a function of the ratio of slow domain ζ . In the slow domain, the moving probability is given as $v_{slow} = 0.1v$. For $\tau = 0.001$, as ζ increases from $\zeta \sim 0$ to $\zeta \sim 0.9$, ρ_I decreases continuously from $\rho_I \sim 0.74$ to $\rho_I \sim 0.4$. For a larger τ , ρ_I also decreases continuously with the rise of ζ but the slope of line becomes gentle.

The above results indicate that, local mobility restriction may inhibit the global spread of epidemic, the effect of which depends on whether there exists global interaction or not. A higher frequency of global interaction will make local mobility restriction become less effective. In figure 4 (b) we plot the relationship between the change of ρ_I , $\Delta\rho_I = \rho_I^{\zeta=0} - \rho_I^{\zeta=0.5}$, and the timescale τ . A log-log relation between $\Delta\rho_I$ and τ , $\Delta\rho_I \sim a'\tau^{-b'}$, in which $a' \sim 1.19 \times 10^{-5}$ and $b' \sim 1.46$, is found. Such results indicate that the ratio of infected individuals is related to the average moving probability. An increase in the ratio of slow domain leads a decrease in the average moving probability and then a decrease in the ratio of infected individuals.

The results in figure 3 and figure 4 indicate that, to make activity domain restriction and local mobility restriction become more effective on epidemic control, we should firstly slow down the frequency of global interaction. Or else, both the epidemic control methods can't play their proper roles.

4. Theoretical analysis

4.1. relationship between epidemic threshold and individual-based random connection

The epidemic threshold is the critical value of infection probability, below which the ratio of infected individuals is small, while above which nearly all the individuals become infected. In a two-dimensional small world network, the epidemic threshold is found to be related to the connection range, the dimension of the lattice and the ratio of shortcuts[42].

In the present model, without the individual-based random connections, which means $\phi = 0$, the epidemic dynamics is similar to that in a regular network. Each individual can only interact with his nearest neighbors, those who are in the same segregated spatial domain or in the nearby domain. The only difference between the evolutionary processes in the two models is that, the encounter probability in the regular network is determined by the connection range, whereas the encounter probability in the present model is determined by population density and moving probability.

As discussed in ref.[42], when there exist a small number of shortcuts, the regular network becomes a small world network. The percolation threshold in the small world network is different from the percolation threshold in the regular network. The percolation threshold in the small world network satisfies the relation $p_c \sim \frac{1}{\phi w}$, in which w is related to the lattice dimension, the connection range along the principal axes and the average cluster size for $\phi = 0$. In the present model, it is found that, for $\phi = 0$, increasing population density and moving probability can both lead to an increase in the encounter probability and then a rise of the ratio of infected individuals. Therefore, the parameter w in the present model should be related to population density and moving probability. For a given spatial size, suppose the parameter w satisfies the relation $w \sim N^\alpha v^\beta$, the epidemic threshold is obtained

$$p_c = \frac{c'}{N^\alpha v^\beta \phi}. \quad (1)$$

In figure 5 (a) and (b) we plot the simulation results of the epidemic threshold as a function of ϕ for a fixed $v = 1$ and $N = 500, 700, 900$, and a fixed $N = 800$ and $v = 0.3, 0.5, 1$. In determining the epidemic threshold p_c , the threshold of the ratio of infected individuals is given as $\rho_I^{th} = 0.95$. From figure 5 we find that the values of p_c calculated from equation (1), in which $c' \sim 56$, $\alpha \sim 1.85$ and $\beta \sim 0.36$, fit the simulation data well, especially for

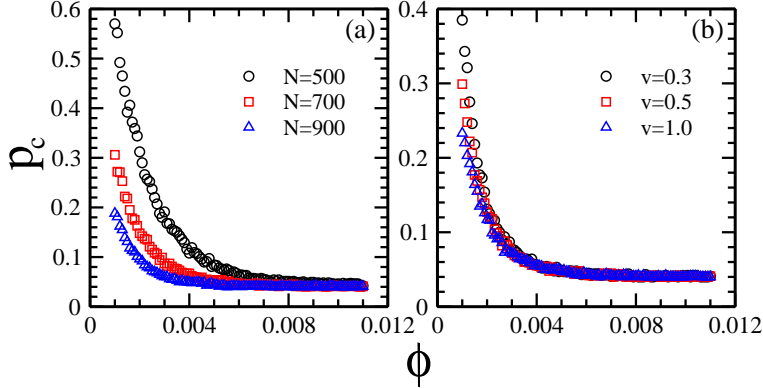


Figure 5: The epidemic threshold as a function of ϕ for (a) $v = 1$ and $N=500$ (circles), 700(squares), 900(triangles); (b) $N = 800$ and $v=0.3$ (circles), 0.5(squares), 1.0(triangles). Final results are averaged over 10 runs. Other parameters are: $\rho_I^{th} = 0.95$, $p_s = 0.001$, $d_x = d_y = 11$, $\tau = 0.5$.

the system with a large value of N and a large value of v . Comparing the results in figure 5 with the results in figure 2, we find that the larger the value of p_c , the smaller the value of ρ_I . The theoretical analysis is in accordance with the simulation data.

4.2. Relationship between encounter time and the size of segregated spatial domain

The propagation speed of epidemic is related to the pairwise interactions between infected individuals and susceptible individuals. If the average encounter time between different individuals is small, it is much easier for the epidemic to break out.

As discussed in ref.[43], on one-dimensional lattice with segregated spatial domains, the average encounter time is determined by the size of segregated domain d_x and the size of overlapping area Δd_x . When there is only one individual in each segregated spatial domain, the average encounter time satisfies the equation[43]

$$\langle t_c^{1d} \rangle = \frac{C(\Delta d_x)^4}{2d_x^2} + \frac{8d_x^2}{\pi} \ln\left(\frac{e^{-\frac{3}{4}}\sqrt{2}d_x}{\Delta d_x}\right), \quad (2)$$

in which $C \sim 0.2116$.

In the present model, as the underlying network changes from one dimensional lattice to two dimensional lattice, both the size of segregated spa-

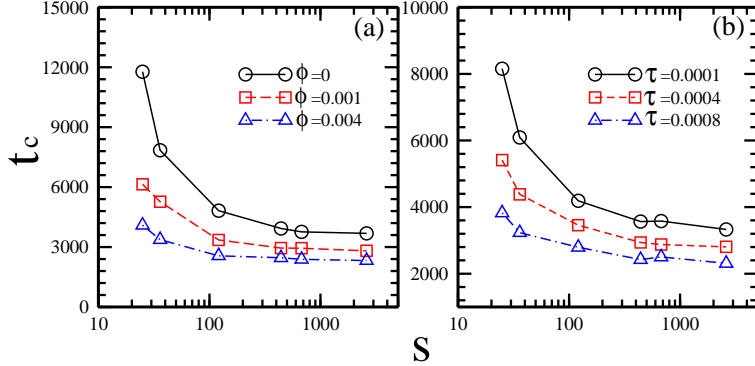


Figure 6: The encounter time as a function of the area of segregated spatial domain for $N = 800$, $p_I = 1$, $p_s = 0$, $v = 0.05$ and (a) $\tau = 0.001$, $\phi=0$ (circles), 0.001(squares), 0.004(triangles); and (b) $\phi = 0.01$, $\tau = 0.0001$ (circles), 0.0004(squares), 0.0008(triangles). Final results are averaged over 50 runs.

tial domain and the size of overlapping area increase. For a given lattice size $L \times L$ and a given population size N , increasing the segregated spatial domain leads to an increase in the number of individuals in each domain, $n = \frac{N}{L \times L} s$. Suppose the average encounter time on two-dimensional lattice is related to the average encounter time on one-dimensional lattice and the number of individuals in each domain, we give an equation

$$\langle t_c \rangle = c_1 + \frac{c_2 \sqrt{\langle t_c^{1d} \rangle}}{n^2}, \quad (3)$$

in which c_1 and c_2 are related to the individual-based random connection ϕ and the timescale τ .

In figure 6 (a) and (b) we plot the simulation results of average encounter time as a function of s for a given $\tau = 0.001$ and different random connection $\phi = 0, 0.001, 0.004$, and a given $\phi = 0.01$ and different timescale $\tau = 0.0001, 0.0004, 0.0008$. The encounter time is obtained as the relaxation time when all the individuals become infected. It is found that the values of t_c calculated from equation (3) fit the simulation data quite well, in which c_1 is related to the value of p_c for $s \rightarrow L \times L$ and c_2 is related to the changing tendency of the line. For a given timescale τ (or random connection ϕ), increasing ϕ (or τ) leads to the decrease of c_1 and c_2 . For example, in figure 6 (a), $c_1 \sim 3800$ and $c_2 \sim 3600$ for $\phi=0$, $c_1 \sim 3000$ and $c_2 \sim 1500$ for $\phi=0.001$, $c_1 \sim 2300$ and $c_2 \sim 850$ for $\phi=0.004$. In figure 6 (b), $c_1 \sim 3400$ and $c_2 \sim 2200$ for $\tau=0.0001$, $c_1 \sim 2800$ and $c_2 \sim 1200$ for $\tau=0.0004$, $c_1 \sim 2400$ and $c_2 \sim 600$

for $\tau=0.0008$.

Comparing the results in figure 6 with the results in figure 3, we find that the larger the value of t_c , the smaller the value of ρ_I . The theoretical analysis is in accordance with the simulation data.

5. Summary

By incorporating segregated spatial domains and individual-based linkage into the SIS model, we investigate the effects of local movement and global interaction on contagion. Compared with the scenario where only random walk or intragroup interaction exists, the coexistence of them leads to a wider spread of epidemic. The effects of activity domain restriction and mobility restriction on epidemic control are extensively investigated. When the global interaction is restricted, both narrowing the segregated spatial domain and reducing local mobility can effectively curb the spread of epidemic. The existence of far away connection makes the epidemic control methods become less effective. A theoretical analysis indicates that the effectiveness of activity restriction on epidemic control depends on the change in average encounter probability and the change in average encounter time. Reducing the ratio of shortcuts and narrowing the activity domain can effectively lead to a decrease in average encounter probability and an increase in average encounter time, and therefore, an increase in epidemic threshold and a decrease in the ratio of infected individuals.

In the future, the coupled effects of mobility patterns and interaction patterns on the evolutionary dynamics will be extensively studied in reaction-diffusion systems and in game models. The time scale effect in these coupled systems should be a favourite of ours.

Acknowledgments

This work is the research fruits of National Natural Science Foundation of China (Grant Nos. 71371165, 11175079, 71471161,71171176), Research Project of Zhejiang Social Sciences Association (Grant No. 2014N079), Collegial Laboratory Project of Zhejiang Province (Grant No. Z201307), Visiting Scholar Project of Teacher Professional Development of Zhejiang Province, Jiangxi Provincial Young Scientist Training Project (Grant No. 20133BCB23017).

References

- [1] M. Tang, L. Liu, and Z. H. Liu, Influence of dynamical condensation on epidemic spreading in scale-free networks, *Phys. Rev. E* 79 (2009) 016108.
- [2] L. X. Zhong, T. Qiu, F. Ren, P. P. Li, and B. H. Chen, Time scales of epidemic spread and risk perception on adaptive networks, *EPL* 94 (2011) 18004.
- [3] M. Boguna, C. Castellano, and R. Pastor-Satorras, Nature of the epidemic threshold for the Susceptible-Infected-Susceptible dynamics in networks, *Phys. Rev. Lett.* 111 (2013) 068701.
- [4] P. Van Mieghem and R. van de Bovenkamp, Non-markovian infection spread dramatically alters the Susceptible-Infected-Susceptible epidemic threshold in networks, *Phys. Rev. Lett.* 110 (2013) 108701.
- [5] Z. H. Liu, X. Wu, H. J. Yang, N. Gupte, B. W. Li, Heat flux distribution and rectification of complex networks, *New J. Phys.* 12 (2010) 023016.
- [6] O. Graser, P. M. Hui, and C. Xu, Separatrices between healthy and endemic states in an adaptive epidemic model, *Physica A* 390 (2011) 906-913.
- [7] K. Gong, M. Tang, P. M. Hui, H. F. Zhang, D. Younghae, and Y. C. Lai, An efficient immunization strategy for community networks, *PLoS One* 8 (2013) e83489.
- [8] F. Schweitzer and L. Behera, Optimal migration promotes the outbreak of cooperation in heterogeneous populations, *Adv. Complex Syst.* 15 (2012) 1250059.
- [9] H. Hong, H. Park, and L. H. Tang, Finite-size scaling of synchronized oscillation on complex networks, *Phys. Rev. E* 76 (2007) 066104.
- [10] V. Belik, T. Geisel, and D. Brockmann, Natural human mobility patterns and spatial spread of infectious diseases, *Phys. Rev. X* 1 (2011) 011001.

- [11] B. Wang, L. Cao, H. Suzuki, and K. Aihara, Safety-information-driven human mobility patterns with metapopulation epidemic dynamics, *SREP* 2 (2012) 00887.
- [12] A. Apolloni, C. Poletto, J. J. Ramasco, P. Jensen, and V. Colizza, Metapopulation epidemic models with heterogeneous mixing and travel behaviour, *Theoretical Biology and Medical Modelling* 11 (2014) 3.
- [13] P. Crepey, F. P. Alvarez, and M. Barthelemy, Epidemic variability in complex networks, *Phys. Rev. E* 73 (2006) 046131.
- [14] J. L. Iribarren and E. Moro, Impact of human activity patterns on the dynamics of information diffusion, *Phys. Rev. Lett.* 103 (2009) 038702.
- [15] M. Tang, Z. H. Liu, B. W. Li, Epidemic spreading by objective traveling, *Europhys. Lett.* 87 (2009) 18005.
- [16] E. Lopez, R. Parshani, R. Cohen, S. Carmi, and S. Havlin, Limited path percolation in complex networks, *Phys. Rev. Lett.* 99 (2007) 188701.
- [17] C. Moore, and M. E. J. Newman, Epidemics and percolation in small-world networks, *Phys. Rev. E* 61 (2000) 5678-5682.
- [18] R. Pastor-Satorras and A. Vespignani, Epidemic spreading in scale-free networks, *Phys. Rev. Lett.* 86 (2001) 3200-3203.
- [19] M. A. Serrano and M. Boguna, Percolation and epidemic thresholds in clustered networks, *Phys. Rev. Lett.* 97 (2006) 088701.
- [20] S. Shao, X. Huang, H. E. Stanley, and S. Havlin, Robustness of a partially interdependent network formed of clustered networks, *Phys. Rev. E* 89 (2014) 032812.
- [21] J. Gao, S. V. Buldyrev, H. E. Stanley, X. Xu, and S. Havlin, Percolation of a general network of networks, *Phys. Rev. E* 88 (2013) 062816.
- [22] Z. Wang, A. Szolnoki, and M. Perc, Self-organization towards optimally interdependent networks by means of coevolution, *New J. Phys.* 16 (2014) 033041.
- [23] A. Saumell-Mendiola, M. A. Serrano, and M. Boguna, Epidemic spreading on interconnected networks, *Phys. Rev. E* 86 (2012) 026106.

- [24] F. Altarelli, A. Braunstein, L. Dall'Asta, A. Lage-Castellanos, and R. Zecchina, Bayesian inference of epidemics on networks via belief propagation, *Phys. Rev. Lett.* 112 (2014) 118701.
- [25] Z. H. Liu and B.B. Hu, Epidemic spreading in community networks, *Europhys. Lett.* 72 (2005) 315-321.
- [26] X. Y. Wu and Z. H. Liu, How community structure influences epidemic spread in social networks, *Physica A* 387 (2008) 623-630.
- [27] Z. H. Liu, Effect of mobility in partially occupied complex networks, *Phys. Rev. E* 81 (2010) 016110.
- [28] Z.M. Yang and T. Zhou, Epidemic spreading in weighted networks: An edge-based mean-field solution, *Phys. Rev. E* 85 (2012) 056106.
- [29] L. Y. Lu, D. B. Chen, and T. Zhou, Small world yields the most effective information spreading, *New J. Phys.* 13 (2011) 123005.
- [30] H. Wang, Q. Li, G. D'Agostino, S. Havlin, H. E. Stanley, and P. Van Mieghen, Effect of the interconnected network structure on the epidemic threshold, *Phys. Rev. E* 88 (2013) 022801.
- [31] Y. Q. Hu, S. Havlin, and H. A. Makse, Conditions for viral influence spreading through multiplex correlated social networks, *Phys. Rev. X* 4 (2014) 021031.
- [32] K. P. Chan, D. F. Zheng, and P. M. Hui, Effects of aging and links removal on epidemic dynamics in scalefree networks, *Int. J. Mod. Phys. B* 18 (2004) 2534-2539.
- [33] M. Dickison, S. Havlin, and H. E. Stanley, Epidemics on interconnected networks, *Phys. Rev. E* 85 (2012) 066109.
- [34] X. F. Fu, L. H. Tang, C.L. Liu, J. D. Huang, T. Hwa, and P. Lenz, Stripe formation in bacterial systems with density-suppressed motility, *Phys. Rev. Lett.* 108 (2012) 198102.
- [35] X. Y. Yan, X. P. Han, B. H. Wang, and T. Zhou, Diversity of individual mobility patterns and emergence of aggregated scaling laws, *Scientific Reports* 3 (2013) 2678.

- [36] V. Colizza and A. Vespignani, Epidemic modeling in metapopulation systems with heterogeneous coupling pattern: Theory and simulations, *Journal of Theoretical Biology* 251 (2008) 450-467.
- [37] N. F. Johnson, C. Xu, Z.Y. Zhao, N. Ducheneaut, N. Yee, G. Tita, and P. M. Hui, Human group formation in online guilds and offline gangs driven by common team dynamic, *Phys. Rev. E* 79 (2009) 066117.
- [38] N. F. Johnson, J. Ashkenazi, Z.Y. Zhao, and L. Quiroga, Equivalent dynamical complexity in a many-body quantum and collective human system, *AIP Advances* 1 (2011) 012114.
- [39] F. Schweitzer, P. Mavrodiev, and C. J. Tessone, How can social herding enhance cooperation? *Adv. Complex Syst.*16 (2013) 1350017.
- [40] M. Perc, J. Gomez-Gardenes, A. Szolnoki, L. M. Floria, and Y. Moreno, Evolutionary dynamics of group interactions on structured populations: A review, *J. R. Soc. Interface* 10 (2013) 20120997.
- [41] T. Fent, P. Groeber, and F. Schweitzer, Coexistence of social norms based on in- and Out-group interactions, *Adv. Complex Syst.*10 (2007) 271-286.
- [42] M. E. J. Newman, I. Jensen, and R. M. Ziff, Percolation and epidemics in a two-dimensional small world, *Phys. Rev. E* 65 (2002) 021904.
- [43] L. Giuggioli, S. Perez-Becker, and D. P. Sanders, Encounter times in overlapping domains: application to epidemic spread in a population of territorial animals, *Phys. Rev. Lett.* 110 (2013) 058103.